IEEE Access
Multidisciplinary | Rapid Review | Open Access Journal

Received October 10, 2018, accepted November 23, 2018, date of publication November 27, 2018,
date of current version December 27, 2018.

Digital Object Identifier 10.1109/ACCESS.2018.2883688

Queue Performance of Energy Harvesting Cognitive Radio Sensor Networks With Cooperative Spectrum Sharing

WANGUO JIAO[1], GUOQING LIU[2], AND HAIQING WU[1]
[1]College of Information Science and Technology, Nanjing Forestry University, Nanjing 210037, China
[2]Key Laboratory of IntelliSense Technology, China Electronics Technology Group Corporation, Nanjing Research Institute of Electronics Technology, Nanjing 210039, China

Corresponding author: Wanguo Jiao (wgjiao87@gmail.com)

This work was supported in part by the National Natural Science Foundation of China under Grant 61701241, in part by the Natural Science Foundation of Jiangsu Province under Grant BK20170935, and in part by the Natural Science Foundation of the Jiangsu Higher Education Institutions of China under Grant 17KJB510030.

ABSTRACT In this paper, we study the queue performance for energy-harvesting cognitive radio sensor networks (EHCRSNs) where the cooperation between the primary user and the sensor is applied. In EHCRSNs, energy harvesting provides a continual energy source for the power-limited sensor, while cognitive radio enables the sensor access the licensed spectrum, which can mitigate the spectrum-scarcity problem of the wireless sensor network. First, with the help of queue theory, we study the queue performance of the EHCRSN and the primary user when the sensor does not assist the service of the primary user. Through analyzing the dynamic energy harvesting and consuming process, we obtain the effect of energy harvesting on the queue performance of the EHCRSN. Then, we further analyze the queue performance when the cooperation between the sensor and the primary user is adopted. Through comparing the result, we observe the effect of energy harvesting on both the performance of the sensor and the primary user and find out the condition under which the cooperation can improve the system performance. The numerical results in different situations further demonstrate the relation between the queue performance and the energy harvesting rate and verify the analysis and the conclusion that the cooperation can improve queue performance under certain conditions. These results are very meaningful for the quality-of-service guarantee in EHCRSNs.

INDEX TERMS Queue performance, energy harvesting, resource sharing, cognitive radio sensor network.

I. INTRODUCTION

The wireless sensor network (WSN), which is often used to collect data for a wide range of applications, becomes a fundamental technology for Big Data [1] and the Internet of Things (IoTs) [2]. Due to constraints of cost and device size, the battery of the sensor often has limited capacity, which results in energy scarcity in the WSN. Hence, how manage limited energy carefully to extend the network lifetime is a crucial problem in the traditional WSN. Available researches have improved the network lifetime effectively, but the lifetime of the network is still bounded due to finite energy supply. To address energy scarcity problem effectively, energy harvesting (EH) technology is adopted by the WSN. By exploiting the EH technology, the sensor can harvest energy from renewable energy sources, such as solar, thermal, wind, and electromagnetic energy. The WSN has continual energy supply. In other words, the energy scarcity problem of the WSN could be solved by using the EH technology, and the sustainability of the network is achieved [3].

Typical WSNs operate on the unlicensed industrial, scientific, and Medical (ISM) band, which has become increasingly crowed due to the massive growth of wireless communication. The increasing crowed ISM band brings severe interference to the data transmission of the WSN, and the spectrum scarcity problem becomes a main limitation of the WSN application. The cognitive radio (CR) technology makes the unlicensed user who uses ISM band opportunistically sense and exploit licensed spectrum. That is, the CR technology can increase transmission opportunity of the unlicensed user and improve the utilization of the

licensed spectrum. By using the CR technology, the WSN can solve the spectrum scarcity problem and improve the quality-of-service (QoS) performance [4].

The integration of EH and CR into WSNs can mitigate both energy and spectrum constraints simultaneously, and such networks are referred to as energy harvesting cognitive radio sensor networks (EHCRSNs) [5], [6]. In EHCRSNs, sensors use the EH technology to obtain energy continuously and work as secondary users to access the licensed spectrum. There are many application scenarios of EHCRSNs, such as smart grid [7] and health monitoring [8].

Although EHCRSNs are spectrum and energy efficient, they face several new challenges comparing with the traditional WSN [9]. First, the energy harvesting process is stochastic and dynamic, which makes balancing energy consumption and energy replenishment challenging. When the energy consuming rate slower or faster than the energy harvesting rate, the energy is underutilization or sensor is failure, respectively [10]. Second, the spectrum utilization by sensors in EHCRSNs has to adapt to the dynamic activity of primary users (PUs), which means not only state of PUs but also the duration of each state. For example, the spectrum occupation of cellular users is in the range of seconds or minutes [11]. When sensors transmit over the channels licensed to cellular users, sensors may have to frequently disrupt their transmissions and switch to a vacant spectrum to avoid collisions with cellular users. Third, the energy harvesting of sensors may occupy idle channel provided by the CR, and the spectrum sensing and channel switch of the CR will consume extra energy collected by the EH. Hence, under these highly correlated stochastic and dynamic conditions, jointly managing energy and spectrum resource for EHCRSNs becomes a challenging task.

Recently, the EHCRSN has been widely studied [5], [6], [12]–[20]. Some of them focus on the resource management to improve network utility. Ren *et al.* [5] designed a joint channel access and sampling rate control scheme to maximize the network utility. Different from [5], Zhang *et al.* [6] proposed an online resource management algorithm, which contains battery management, sampling rate control, and channel allocation, to maximize the aggregate network utility while guarantee the requirement of the licensed subscriber and balance the energy consumption. The network utility was also optimized by an online algorithm which manages available energy and unoccupied licensed spectrum in [12]. Despite optimizing network utility, some researchers work on the throughput of the EHCRSN. In [13], a spectrum access scheme was proposed to maximize the service rate of the sensor and optimize the end-to-end throughput of the multi-hop EHCRSN in [14]. Under the assumption that the sensor cannot work as energy collector and data sender simultaneously, the optimal mode selection policy was proposed in [15] to maximize an expected total throughput of the system. Outage probability is another key metric of network performance, which has been widely studied in EHCRSNs. In [21], the outage probabilities of the primary user and the sensor were analyzed, and the relation between the outage probability and channel parameters was also studied. The transmission outage probability of the cognitive wireless sensor network was improved by using the optimal relay selection policy designed by [16]. The outage probability of the EHCRSN was minimized in [17]. Literature [18] maximized the overall success probability of the network through allocating the transmit power for the sensor and the primary user. There are also some works on the self-sustainability of the EHCRSN. Such as the scheme proposed in [19] can effectively extend the network lifetime through selecting the optimal sensing nodes for cooperative spectrum sensing, while a joint of the spectrum sensor scheduling and the data sensor resource allocation designed in [20] can maintain the sustainability of the EHCRSN.

The above-mentioned literatures can effectively improve network performance metrics of the EHCRSN by digging the potential of the EH technology and the CR technology. However, there is little work on the QoS performance of the EHCRSN. In [21], the outage probability of the system with cooperative spectrum sharing was analyzed. Other QoS performance, such as queue length and waiting time, has not been well studied in the EHCRSN. To fill this research gap, we will analyze the queue performance of both the sensor in the EHCRSN and the primary user.

The cooperation between the secondary user and the primary user is widely used in the CR system [22]. In EHCRSNs, through assisting the service of the primary user to shorten the occupation time of the licensed spectrum, the sensor can gain more transmission opportunity and improve the service quality. Furthermore, this cooperation may reduce the transmission time of primary user and increase the data transmission rate, and then the spectrum efficiency of the system is improved. However, the cooperation will consume extra energy of the sensor to help the primary user. This requires that sensor in the EHCRSN continually gather ambient energy to guarantee its own energy supply. Hence, it is important for the EHCRSN that the sensor whether can obtain more transmission chance by consuming extra energy to improve the performance. In this paper, we will study the queue performance of the EHCRSN when the cooperation is applied. There are many cooperation manners in the CR system. We consider a typical cooperation scheme where the sensor works as a relay of the primary user in this work.

In this paper, we propose an analytical method for studying queue performance of EHCRSNs. First, we consider a typical EHCRSN where the sensor just works as a secondary user. Through modeling the system by a preemptive queue system with two priorities and studying the state of the battery with a stochastic energy harvesting process, we derive expressions of average queue length and average delay of both the primary user and the sensor. Based on the analysis of the system without cooperation, we further study the queue performance of the system with cooperation and propose a two dimensional Markov chain to describe the queue state

of the sensor. Through solving the Markov chain, we obtain the queue performance of the system with the cooperation. Afterwards, we further compare the results of these two different systems, and find out the condition under which the spectrum sharing should be used and the relation between the queue performance and system parameters.

The rest of this paper is organized as follows. In Section II, the system model is described. Section III analyzes the queue performance of the system without cooperation. In Section IV, the system with cooperative spectrum sharing is studied. The numerical result and the comparing of the queue performance are given in Section V. Finally, we conclude this paper in Section VI.

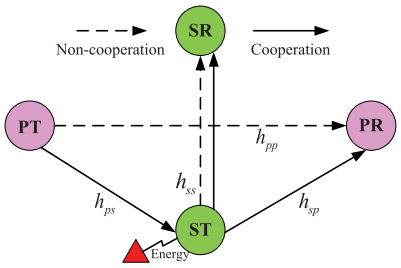

FIGURE 1. System model.

II. SYSTEM MODEL

Consider a single-hop slotted EHCRSN which consists of a pair sensor nodes: ST and SR. For simplicity, the length of each slot is normalized as 1. The EHCRSN coexists with a pair of primary users, denoted by PT and PR, which have the privilege to access the licensed spectrum. As shown in Fig. 1, links from PT to PR, from ST to SR, from PT to ST, and from ST to PR are denoted by h_{pp}, h_{ss}, h_{ps}, and h_{sp}, respectively. All of these four links are the Rayleigh fading channel and the probability distribution function (PDF) of the received signal-to-noise ratio (SNR) at the receiver can be expressed as

$$f_{xy}(\gamma) = \frac{1}{\bar{\gamma}_{xy}} \exp(-\frac{\gamma_{xy}}{\bar{\gamma}_{xy}}), \tag{1}$$

where γ_{xy} is the received SNR, $\bar{\gamma}_{xy}$ is the average received SNR, and xy represents pp, ss, ps, or sp.

The traffic arrival process of the primary user is a Poisson process with λ_p. During each slot, the sensor generates a packet with probability λ_s. Hence, the packet arrival intervals of the sensor obey the geometric distribution of parameter $1/\lambda_s$. All arriving packets are stored in the corresponding buffer with infinite size. The queue service discipline of each user is first-in-first-out.

At the physical layer, the transmitter adopts a certain modulation and coding scheme, thus the data rate of each channel is constant. Then, the transmission time of each packet is constant too. To simplify analysis, we assume that the transmission time of each packet is one slot. As the wireless channel is time varying, the packet transmission may be fail due to poor channel condition. In this paper, we assume that the packet transmission is fail if the received SNR is smaller than the received threshold. The received thresholds of PR, ST, and SR are γ_p, γ_{ps}, and γ_s, respectively. For each transmitter-receiver pair, the probability that a packet transmission is successful can be calculated similarly. Thus, we take a random transmission pair as the example to derive the expression of the successful transmission probability, such as the pair of PT and PR.

According to the PDF of the received SNR, the successful probability $\beta_p(t)$ of the packet transmission at the t-th slot can be calculated as $\beta_p(t) = \Pr(\gamma_{pp}(t) > \gamma_p)$, where $\gamma_{pp}(t)$ is the received SNR of PR at the t-th slot. Since the packet transmission is over a Rayleigh fading channel and the Rayleigh fading channel has memoryless property, the received SNR is independent at each slot. That is, the received SNR has the same distribution at each slot, which is given in (1). Hence, the packet transmission has the same successful probability in each slot. We omit t in the following and the successful probability β_p of the packet transmission can be calculated as

$$\beta_p = \Pr(\gamma_{pp} > \gamma_p) = \exp(-\frac{\gamma_p}{\bar{\gamma}_{pp}}), \tag{2}$$

The successful probabilities of other transmission pairs can be calculated similarly by using (2). To guarantee the reliability of the packet transmission, the automatic repeat request (ARQ) is used at the data link layer. If a packet transmission fails, this packet will be retransmitted at the next available slot until the packet is successfully received by the receiver.

In this paper, we consider an EHCRSN where the CR technology and the EH technology are adopted. These two technologies will affect the queue performance of the sensor. In the following, we will introduce the operation mode of the sensor as the secondary user and the energy harvesting model used in our work.

A. OPERATION MODE

In this paper, we will compare the queue performance of system when the primary user and the sensor work in two different modes: non-cooperation and cooperation. Each mode will be illustrated in detail as follows.

1) NON-COOPERATION MODE

In non-cooperation mode, sensors in the EHCRSN work as interweave paradigm [23]. In interweave paradigm, the sensor opportunistically uses the licensed spectrum which is not occupied by the primary user. To obtain the occupation information, the sensor should sense spectrum state by using spectrum sensing technology. In this paper, we assume that the spectrum sensing result is perfect and both the time and energy consumed by the spectrum sensing are ignored. That is, there is not collision or interfering between the primary user and the sensor.

In this mode, the packet of the primary user is directly transmitted from PT to PR. If the channel between PT and PR is active, then ST cannot serve its buffered packets.

We assume that each packet transmission starts at the beginning of a slot. Hence, if a new packet of the primary user arrives during the current slot, this packet only can be served at the beginning of the next slot no matter whether the sensor is transmitting packets or not. Therefore, the service process of the sensor does not affect the service process of the primary user. From the primary user point of view, the sensor appears to be nonexistent.

2) COOPERATION MODE

In cooperation mode, the sensor helps packet transmission of the primary user to get more transmission opportunity. The sensor still works in the interweave paradigm. As shown in Fig. 1, PT first sends packets to ST, then if ST has enough energy and the buffer of PT is empty, ST transmits packets which come from PT to PR. All packets from PT are sent to PR, then ST starts to serve its own generated packets.

In this mode, the packet service of the primary user can be divided into two stages: from PT to ST and from ST to PR. As the primary user has the higher priority, the performance of the second stage relays on the service process of the first stage. Moreover, the performance of the second stage is also influenced by the channel condition between ST and PR and the energy harvesting process of the sensor. Therefore, the cooperation makes the packet service processes correlate with each other and the correlation is very complicated.

B. ENERGY HARVESTING PROCESS

We assume that the sensor in the EHCRSN can transmit packets and collect energy simultaneously. In each slot, the sensor harvests energy from the ambient sources, such as wind, solar, electromagnetic wave. We assume that the energy harvesting process is a stationary random process, and the amount of collecting energy in different slots are independent identically distributed (i.i.d.) exponential random variables. As the transmitter adopts a fixed modulation and coding scheme, the energy consumed by a packet transmission is constant. Hence, in this paper, the unit of the harvesting energy is the packet and the energy packet is defined as the amount of energy which is enough to transmit a packet. As amounts of collecting energy in each slot is an i.i.d. exponential random variable, the energy harvesting process is a Bernoulli process with p_e. To simplify the analysis, we assume that the capacity of the battery storing the collected energy is infinite.

III. NON-COOPERATION MODE

In this section, we consider there is no cooperation between the primary user and the sensor. When the primary user has packets, it transmits on the spectrum, and the sensor should leave the spectrum immediately. Hence, the primary user has higher priority, and the service rule of the primary user and the sensor is the preemptive resume priority discipline with two priorities. Since the service of the higher-priority user will not be influenced by the lower-priority user, the queue performance of the primary user can be analyzed independently.

The packet arrival process is a Poisson process with rate λ_p, and the primary user can be represented by an M/G/1 queueing system. According to the Pollaczek-Khinchin (P-K) formula, the average queue length is expressed as

$$N_{PT-N} = \frac{\lambda_p^2 E[X_{PT-N}^2]}{2(1-\rho_{PT-N})}, \tag{3}$$

where $\rho_{PT-N} = \lambda_p E[X_{PT-N}]$, X_{PT-N} is the packet service time of the primary user, $E[X]$ and $E[X^2]$ are the mean value and the second moment of variable X, respectively.

As the channel between PT and PR is a Rayleigh fading channel, the successful transmission probability is independent in different slots. Moreover, the packet unsuccessfully received will be retransmitted in the next slot. Hence, the packet service time X_{PT-N} obeys a geometric distribution. The successful transmission probability has been given in (2), and the average packet service time $E[X_{PT-N}]$ can be calculated as

$$\begin{aligned} E[X_{PT-N}] &= \beta_p + 2\beta_p(1-\beta_p) + 3\beta_p(1-\beta_p)^2 + \cdots \\ &= \frac{1}{\beta_p}. \end{aligned} \tag{4}$$

Similarly, the second moment of X_{PT-N} is

$$E[X_{PT-N}^2] = \sum_{n=1}^{\infty} n^2 \beta_p (1-\beta_p)^{n-1} = \frac{1-\beta_p}{\beta_p^2}. \tag{5}$$

According to Little theory, the average delay T_{PT-N} of the primary user's packets can be calculated as

$$\begin{aligned} T_{PT-N} &= E[X_{PT-N}] + \lambda_p N_{PT-N} \\ &= \frac{1}{1-\rho_{PT-N}} E[X_{PT-N}]. \end{aligned} \tag{6}$$

As the sensor has lower priority, the average delay T_{ST-N} of the sensor's packets contains three parts: the average service time $E[X_{ST-N}]$, the average time $E[R]$ required to serve packets which have been in the system when a new packet of the sensor arrives, and the average waiting time for packets of the primary user which arrive during serving the packet of the sensor. As the packet arrival process of the primary user is a Poisson process with rate λ_p and the average packet service time of the primary user is $E[X_{PT-N}]$, the third part is $\lambda_p T_{ST-N} E[X_{PT-N}]$. That is, the third part is $\rho_{PT-N} T_{ST-N}$. Similar to the derivation of the residual time of the M/G/1 system [24], the second part $E[R]$ can be calculated as

$$E[R] = \frac{\frac{1}{2}\left(\lambda_p E[X_{PT-N}^2] + \lambda_s E[X_{ST-N}^2]\right)}{1-\rho_{PT-N}-\rho_{ST-N}}, \tag{7}$$

where $\rho_{ST-N} = \lambda_s E[X_{ST-N}]$.

Therefore, the average delay T_{ST-N} is derived as

$$T_{ST-N} = E[X_{ST-N}] + E[R] + \rho_{PT-N} T_{ST-N}. \tag{8}$$

By substituting (7) into (8), T_{ST-N} can be further written as

$$\begin{aligned} T_{ST-N} = {} & \frac{E[X_{ST-N}]}{1-\rho_{PT-N}} \\ & + \frac{\lambda_p E[X_{PT-N}^2] + \lambda_s E[X_{ST-N}^2]}{2(1-\rho_{PT-N}-\rho_{ST-N})(1-\rho_{PT-N})}. \end{aligned} \tag{9}$$

Similarly, by using T_{ST-N}, the average queue length of the sensor can be obtained, which is

$$N_{ST-N} = \lambda_s(T_{ST-N} - E[X_{ST-N}]). \tag{10}$$

From (9) and (10), it can be found that the queue performance of the sensor would be obtained if $E[X^2_{ST-N}]$ and $E[X_{ST-N}]$ are known. To derive $E[X^2_{ST-N}]$ and $E[X_{ST-N}]$, we will study the service process of the sensor in the following.

For the sensor, the packet transmission starts when two conditions are satisfied. One is that the buffer of the primary user is empty. The expressions of T_{ST-N} and N_{ST-N} in (9) and (10), respectively, have considered the effect of this condition. The other is there is enough energy for transmitting a packet. If the sensor does not have enough energy in the battery, it cannot transmit packets. Hence, the packet service time is related to the state of the battery, especially, the probability of the nonempty battery. To obtain the probability that the battery of the sensor is nonempty, we will analyze the energy harvesting and consuming process of the sensor.

As the energy harvesting process is a Bernoulli process with p_e, the battery can be described by a one-dimensional Markov chain. State $S(t)$ of the corresponding Markov chain is the number of energy packets in the battery at the t-th slot. The transition diagram of the Markov chain is shown in Fig. 2.

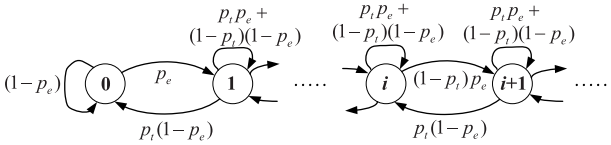

FIGURE 2. The Markov chain of the energy state.

As the service time of the primary user obeys a geometric distribution and the packet arrival process of the sensor is a Bernoulli process, the energy consuming process of the sensor is a Bernoulli process. Furthermore, the energy arrival process is also a Bernoulli process, hence the Markov chain constructed by $S(t)$ is a stationary Markov chain and the transmission probability $\Pr(S(t+1) = j | S(t) = i)$ can be abbreviated as P_{ij}. The calculation of the transition probability P_{ij} can be divided into two cases: $i = 0$ and $i \neq 0$.

Firstly, we consider the case with $i = 0$, which means the battery of the sensor is empty. There are two possible states in the next slot: $S = 1$ or $S = 0$. Since the battery is empty, the sensor cannot transmit packets due to energy shortage, and then the consumed energy of the current slot is 0. According to energy harvesting process and energy consuming process, if one energy packet is collected, then $S = 1$; otherwise $S = 0$. Hence, the transition probabilities in this case can be calculated as

$$P_{01} = p_e \quad \text{and} \quad P_{00} = 1 - p_e. \tag{11}$$

When $i \neq 0$, there are three possible states in the next slot: $S = i - 1$, $S = i$, or $S = i + 1$. If there is one packet be transmitted and no energy packets be collected, then $S = i-1$. Similarly, If there is no packet be transmitted and an energy packet be collected, then $S = i + 1$. Otherwise, the next state is $S = i$. Thus, the transition probability of this case is

$$P_{i(i-1)} = p_t(1 - p_e), \quad P_{i(i+1)} = p_e(1 - p_t),$$

and

$$P_{ii} = p_e p_t + (1 - p_t)(1 - p_e), \tag{12}$$

where p_t is the probability that the sensor transmits the packet in a random slot.

If the spectrum is occupied by the primary user or the buffer of the sensor is empty, the sensor does not transmit. Thus, p_t can be expressed as

$$p_t = (1 - P_0)(1 - \rho_{PT-N})\rho_{ST-N}, \tag{13}$$

where P_0 is the probability that the battery is empty.

We assume that the battery can achieve steady state, otherwise $P_0 = 0$ and the system can be simplified as the sensor always has enough energy. Let P_i denote the probability that there are i energy packets in the battery. According to Markov theory, if the system achieves the steady state, the probability from state 1 to state 2 equals to the probability from state 2 to state 1. Hence, P_i and P_{ij} satisfy

$$\begin{aligned} P_0 p_e &= P_1 p_t(1 - p_e), \\ P_i p_e(1 - p_t) &= P_{i+1} p_t(1 - p_e), \quad i = 1, 2, 3, \cdots \end{aligned} \tag{14}$$

Through solving equations in (14), the steady-state probability P_i can be derived as

$$P_0 = p_t - p_e, \quad \text{and } P_i = \rho_e^{i-1} \frac{p_e}{p_t(1 - p_e)} P_0, \quad i = 1, 2, \cdots \tag{15}$$

where $\rho_e = \frac{p_e(1-p_t)}{p_t(1-p_e)}$. By substituting (13) into (15), P_0 is calculated, and the probability of the nonempty battery expressed as $1 - P_0$ is obtained.

Based on P_0, we derive expressions of $E[X^2_{ST-N}]$ and $E[X_{ST-N}]$. For the sensor, one successful transmission requires two conditions: there is enough energy and the received SNR is larger than the SNR threshold. According to (2), the probability that the received SNR is larger than the SNR threshold can be calculated as $\beta_s = \Pr(\gamma_{ss} > \gamma_s) = \exp(-\gamma_s/\bar{\gamma}_{ss})$. As the ARQ is adopted, if the packet is not received by SR successfully, it will be retransmitted until it is received successfully. If the first transmission of a packet is successful, the packet service time is one slot. As the effect of the primary user has been considered, when the received SNR is larger than threshold and there is enough energy in the battery, the packet transmission is successful. Hence, the probability that the packet service time equals to one slot is $\beta_s(1-P_0)$. Similarly, the probability that the packet service time of the sensor is i slots is calculated as q_i, which is given in Table 1. Table 1 lists the probability mass function (PMF) of X_{ST-N}, where $\binom{n}{m}$ is the combination function.

By using the PMF in Table 1, $E[X_{ST-N}]$ and $E[X^2_{ST-N}]$ can be calculated by $E[X_{ST-N}] = \sum_{i=1}^{\infty} i q_i$ and

TABLE 1. The PMF of the sensor's packet service time.

X_{ST-N}	Probability (q_i)
1	$(1-P_0)\beta_s$
2	$P_0\left[(1-p_e)p_e\beta_s+p_e^2(1-\beta_s)\beta_s\right]+P_1(1-\beta_s)\left[p_e\beta_s+(1-p_e)p_e\beta_s\right]+P_2(1-\beta_s)\beta_s$
...	...
i	$\beta_s\sum_{n=0}^{i}P_n(1-\beta_s)^n\sum_{m=0}^{i-n+1}(1-\beta_s)^m\sum_{k=m+1}^{n}\binom{n}{m}p_e^k(1-p_e)^{n-k}$
...	...

$E[X_{ST-N}^2]=\sum_{i=1}^{\infty}i^2\,q_i$, respectively, where q_i is the probability that the packet service time of the sensor is i slots. By substituting $E[X_{ST-N}]$ and $E[X_{ST-N}^2]$ into (9) and (10), the queue performance of the sensor is obtained.

IV. COOPERATION MODE

In this section, the sensor works as a relay of the primary user to earn more transmission chances. Due to energy constraint and the criterion of opportunistic spectrum access, the sensor cannot transmit the received packet of the primary user immediately if it does not have enough energy or the primary user continues transmitting. To differentiate packets from different sources, packets received from the primary user and generated by the sensor are stored in different queues. Two queues in the ST are denoted by $ST1$ and $ST2$, which are used to store packets from the PT and packets generated by the sensor, respectively. Hence, in the cooperative system, there are three packet queues, and the relation among three queues is shown in Fig. 3.

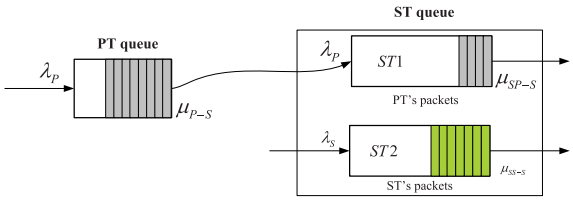

FIGURE 3. Queue model of the system with the cooperation.

Firstly, we analyze the queue in the primary user, which is denoted by PT queue. When the system works in cooperation mode, the primary transmitter still has higher priority. That is, if the buffer of PT is nonempty, it will transmit buffered packets at the beginning of a slot, no matter the ST serves $ST1$ or $ST2$. Hence, the queue of the primary user and queues of the sensor construct a preemptive resume queue system with two priority users. As PT has higher priority, the performance of the PT queue in cooperation mode can be analyzed similarly as the queue performance of the primary user in non-cooperation mode.

Referring to (3) and (6), the average queue length N_{PT-Cp} of PT queue and the average delay T_{PT-Cp} of packets in PT queue can be obtained as

$$N_{PT-Cp}=\frac{\lambda_p^2(1-\beta_{ps})}{2\beta_{ps}(\beta_{ps}-\lambda_p)}, \tag{16}$$

$$T_{PT-Cp}=\frac{1}{\beta_{ps}-\lambda_p}, \tag{17}$$

where β_{ps} is the successful probability of packet transmission from PT to ST. According to (2), β_{ps} can be calculated as $\beta_{ps}=\exp(-\gamma_{ps}/\bar{\gamma}_{ps})$.

Based on the analysis of PT queue, we will analyze two queues in the ST as follows. As shown in Fig. 3, the packet departure process of PT queue is the packet arrival process of $ST1$. From the analysis of queue performance of the primary user in Section III, the packet service process of the primary user has the memoryless property. According to Burke's Theorem, the departure process of PT queue is a Poisson process with λ_p, and numbers of packets in PT queue and in $ST1$ are independent of the sequence of departure times at each time. That is, the packet arrival process of $ST1$ is a Poisson process with λ_p and the state of $ST1$ is independent of PT queue. Hence, arrival processes of two queues at the ST are a Poisson process with λ_p and a Bernoulli process with λ_s, respectively.

As these two queues share one energy queue and one authorized spectrum and packets from PT have higher priority, they construct another preemptive resume queue system with two priority users. However, in this preemptive resume queue system, the arrival process and the service process of $ST1$ is no longer independent with each other. This is because packets in $ST1$ is from PT, and PT queue shares the spectrum with $ST1$. Therefore, the performance of $ST1$ and $ST2$ cannot be calculated as in non-cooperation mode.

To study the performance of two queues in the ST, we are turning to Markov theory. First, we let $\mathbf{Q}(t)=[Q_1(t),Q_2(t)]$ denote queue lengths of $ST1$ and $ST2$ at the beginning of the t-th slot. Given $\mathbf{Q}(t)$, $Q_1(t+1)$ and $Q_2(t+1)$ are only related to the arrival process and the service process. The service process of $\mathbf{Q}(t)$ is determined by the spectrum state and the state of the energy queue. According to the analysis in Section III, the spectrum state, which manifests as the spectrum is occupied by the primary user or not, in each slot is independent. In addition, from the analysis of the energy

harvesting and consuming process, the state of the energy queue also has the memoryless property. Hence, the service of $\mathbf{Q}(t)$ is not affected by the history information of the system. Meanwhile, it has been discussed that arrival processes of $ST1$ and $ST2$ also have the memoryless property. Therefore, the Markov property holds, and $\mathbf{Q}(t)$ can be modeled by a two-dimensional discrete time Markov chain (DTMC). Before solving the two-dimensional DTMC, we study the property of the proposed DTMC. Referring to [25], it can be found that the proposed Markov chain is a homogeneous, irreducible, and aperiodic DTMC. Hence, the state transition of the DTMC is timeless, and $\mathbf{Q}(t)$ can be simplified as $\mathbf{Q} = [Q_1, Q_2]$. The state (i, j) of the DTMC means $Q_1 = i$ and $Q_2 = j$.

The one-step transition matrix of $\mathbf{Q}$ is defined as $\mathbf{q} = \{q_{(i,j)}^{(k,l)}\}$, where $q_{(i,j)}^{(k,l)}$ is the probability of the transition from the state (i, j) to state (k, l). According to [26], if a Markov chain is a homogeneous, irreducible, and aperiodic DTMC, then there is one and only one steady-state solution which can be obtained by solving balance equations. The proposed two-dimensional Markov chain is a homogeneous, irreducible, and aperiodic DTMC, thus there is only one stationary distribution of $\mathbf{Q}$, which satisfies the following equations

$$\boldsymbol{\pi}\mathbf{q} = \boldsymbol{\pi}, \quad \boldsymbol{\pi}\mathbf{e} = 1, \tag{18}$$

where $\mathbf{e}$ is the unit vector and $\boldsymbol{\pi}$ is the stationary probability of $\mathbf{Q}$. The i-th element of $\boldsymbol{\pi}$ is $\Pr(Q_1 = i_1, Q_2 = i_2)$. Equation (18) indicates that $\boldsymbol{\pi}$ can be obtained through deriving matrix $\mathbf{q}$ and solving linear equations in (18).

As $ST1$ has higher priority, $ST2$ cannot have service chance when $ST1$ is not empty. Hence, we divide the derivation of $\mathbf{q}$ into two cases: $Q_1 = 0$ and $Q_1 \neq 0$.

Case A: $Q_1 = 0$

Without loss of generality, we assume that the queue system is in state $(0, j)$. Through analyzing transitions among state $(0, j)$ and other states, the transmission probabilities of this case can be derived. As the buffer storing PT's packets is empty at the current slot and PT can only transmit one packet during a slot, Q_1 can be 0 or 1 in the next slot. Similarly, Q_2 may be $j + 1$, j, or $j - 1$ in the next slot. However, when PT serves packets, ST cannot transmit. That is, $Q_1 = 1$ and $Q_2 = j - 1$ in the next slot is impossible. Thus, the state at the next slot may be $(0, j-1)$, $(0, j)$, $(0, j+1)$, $(1, j)$ or $(1, j+1)$. Similarly, except $(1, j+1)$, transitions from these states and state $(1, j-1)$ to state $(0, j)$ are also possible. Therefore, transitions among state $(0, j)$ and other states are shown in Fig. 4.

The calculation of the probability of the transition from other states to state $(0, j)$ is similar to the transition probability of the state $(0, j)$ to other states. From Fig. 4, it can be found that the transition probabilities of this case can be obtained if expressions of $q_{(0,j)}^{(0,j)}$, $q_{(0,j)}^{(0,j-1)}$, $q_{(0,j)}^{(0,j+1)}$, $q_{(0,j)}^{(1,j)}$, and $q_{(0,j)}^{(1,j+1)}$ are derived.

At the current slot, the queue state is $(0, j)$, if the buffer of PT is empty, $ST2$ will have service chance; otherwise

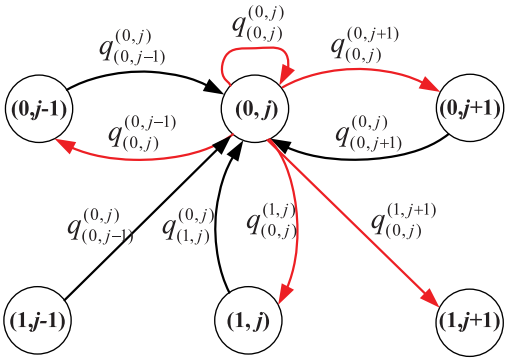

FIGURE 4. The one-step transitions related with state $(0, j)$.

PT will occupy the spectrum and transmit packets to ST. Hence, we will study two possible situations respectively. First, we consider PT has packets. According to the above analysis, the probability that the buffer of PT is nonempty is $\rho_{PTc} = \lambda_p/\beta_{ps}$. When PT has packets, if the packet transmission of PT fails, the length of $ST1$ will be still 0, otherwise the length of $ST1$ will become 1. The probability that the packet transmission of PT is successful is β_{ps}. Since PT occupies the spectrum, ST cannot serve packets. Hence, if ST generates a packet, the state of $ST2$ will change to $j+1$, otherwise it will be still j. If the buffer of PT is empty, $ST1$ can be only one state 0, and ST will serve packets in $ST2$.

A successful packet transmission from ST to SR should satisfy two conditions: one is the received SNR is larger than the received threshold, and the other is ST has enough energy. Based on the analysis of energy state at ST in Section III, the probability P_{ec} that the battery of the sensor is nonempty in cooperation mode can be calculated similarly. Then, the successful probability of packet transmission from ST to SR can be expressed as $\alpha_s = P_{ec}\Pr(\gamma_{ss} > \gamma_s) = P_{ec}\exp(-\gamma_s/\bar{\gamma}_{ss})$.

According to above analysis, there are three possible situations result in the next state being $(0, j)$. These three situations are: PT does not have packets, ST generates a packet and transmits a packet to PR successfully; PT does not have packet, ST does not generate new packets, and the packet transmission from ST to SR fails; PT has packets, the packet transmission from PT to ST fails, and ST does not generate new packets. The probabilities of these three situations are $(1 - \rho_{PTc})\lambda_s\alpha_s$, $(1 - \rho_{PTc})(1 - \lambda_s)(1 - \alpha_s)$, and $\rho_{PTc}(1 - \lambda_s)(1 - \beta_{ps})$, respectively. Hence, the transition probability from state $(0, j)$ to state $(0, j)$ can be calculated as

$$q_{(0,j)}^{(0,j)} = (1 - \rho_{PTc})[\lambda_s\alpha_s + (1 - \lambda_s)(1 - \alpha_s)] + \rho_{PTc}(1 - \beta_{ps})(1 - \lambda_s). \tag{19}$$

There is only one situation makes the state at the next slot is $(0, j-1)$. The situation is that the buffer of PT is empty and ST does not generate new packets and successfully transmits a packet to SR. Thus the transition probability from state $(0, j)$

to state $(0, j-1)$ is

$$q_{(0,j)}^{(0,j-1)} = (1-\rho_{PTc})(1-\lambda_s)\alpha_s. \tag{20}$$

From state $(0, j)$ to state $(0, j+1)$, there are two possible situations: one is that the buffer of PT is empty, ST does not generate new packets, and the packet transmission of ST is unsuccessful; the other is that PT has packets, the packet transmission of PT fails, and ST generates a new packet. Considering these two situations, the transition probability from state $(0, j)$ to state $(0, j-1)$ is derived as

$$q_{(0,j)}^{(0,j+1)} = (1-\rho_{PTc})\lambda_s\alpha_s + \rho_{PTc}(1-\beta_{ps})\lambda_s \tag{21}$$

At the next slot, $ST1 = 1$ means that PT has packets and transmits a packet to ST successfully. If ST generates a new packets, the state at the next slot will be $(1, j+1)$, otherwise, the state will be $(1, j)$. Hence, the transition probabilities from state $(0, j)$ to state $(1, j)$ and state $(1, j+1)$ are

$$q_{(0,j)}^{(1,j)} = \rho_{PTc}\beta_{ps}(1-\lambda_s), \tag{22}$$

and

$$q_{(0,j)}^{(1,j+1)} = \rho_{PTc}\beta_{ps}\lambda_s, \tag{23}$$

respectively.

So far, the transition probabilities from state $(0, j)$ to other states are derived. Similarly, probabilities of other transitions related with state $(0, j)$ can be calculated similarly.

Case B: $Q_1 \neq 0$

When $Q_1 \neq 0$, $ST2$ cannot get service chance. Hence, if Q_2 is j at the current slot, it can only be j or $j+1$ at the next slot. Similar to the analysis of **Case A**, if $Q_1 = i$ at the current slot, the queue length of $ST1$ could be $i-1$, i, or $i+1$, which is determined by the state of the buffer at PT, channel quality of PT-ST pair and ST-SR pair. Take state (i, j) as an example, we demonstrate the derivation of transition probabilities in this case, and transitions among state (i, j) and other states are shown in Fig. 5.

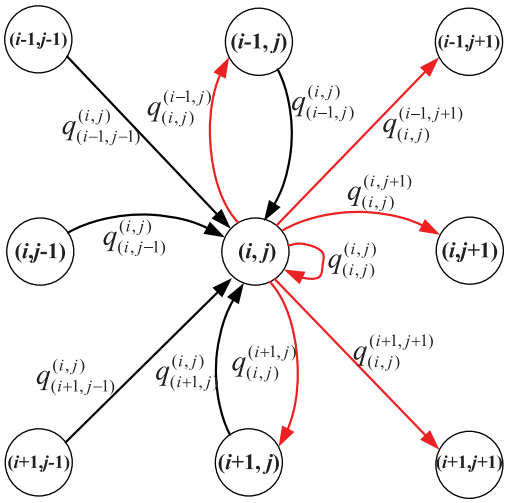

FIGURE 5. The one-step transitions related with (i, j).

First, we consider the situation that the queue state of $ST1$ is unchanged. If the buffer of PT is empty and the packet transmission from ST to PR fails, the queue length of $ST1$ will remain unchanged. Besides, when PT has packets and sends a packet to ST unsuccessfully, $ST1$ keeps in the same state. As the length of $ST1$ is larger than 0, the length of $ST2$ remains the same when ST does not generate a packet while changes into the other value if ST generates a packet. Therefore, the transition probabilities from state (i, j) to state (i, j) and to state $(i, j+1)$ are

$$q_{(i,j)}^{(i,j)} = \left[(1-\rho_{PTc})(1-\alpha_p) + \rho_{PTc}(1-\beta_{ps})\right](1-\lambda_s), \tag{24}$$

and

$$q_{(i,j)}^{(i,j+1)} = \left[(1-\rho_{PTc})(1-\alpha_p) + \rho_{PTc}(1-\beta_{ps})\right]\lambda_s, \tag{25}$$

respectively, where α_p is the successful probability of the packet transmission from ST to PR. Similar to α_s, α_p can be calculated as $\alpha_p = P_{ec}\exp(-\gamma_s/\bar{\gamma}_{sp})$.

If ST receives a packet from PT successfully, the length of Q_1 will change into $i+1$. A successful packet transmission from PT to ST indicates that PT has packets and the received SNR of ST is larger than the received threshold. The corresponding probability is $(1-\rho_{PTc})\beta_{ps}$. The probabilities of transitions from state (i, j) to state $(i+1, j)$ and to state $(i+1, j+1)$ can be expressed as

$$q_{(i,j)}^{(i+1,j)} = \rho_{PTc}\beta_{ps}(1-\lambda_s), \tag{26}$$

and

$$q_{(i,j)}^{(i+1,j+1)} = \rho_{PTc}\beta_{ps}\lambda_s, \tag{27}$$

respectively.

Similarly, the packet transmission from ST to PR is successful, the length of Q_1 will become $i-1$. This is because ST sends packets to PR only when the buffer of PT is empty, and then there is no new packet arrives in $ST1$. Thus, the probability that the length of Q_1 changes from i to $i-1$ is $(1-\rho_{PTc})\alpha_p$. Then, the probabilities that the state (i, j) transits to state $(i-1, j)$ and state $(i-1, j+1)$ are derived as

$$q_{(i,j)}^{(i-1,j)} = (1-\rho_{PTc})\alpha_p(1-\lambda_s), \tag{28}$$

and

$$q_{(i,j)}^{(i-1,j+1)} = (1-\rho_{PTc})\alpha_p\lambda_s, \tag{29}$$

respectively.

By using (24)-(29), other transition probabilities can be calculated similarly. By combining the results in two cases, we obtain the transition matrix $\mathbf{q}$. Substituting $\mathbf{q}$ into (18), the stationary probability $\boldsymbol{\pi}$ of $\mathbf{Q}$ is obtained by solving the linear equations. Based on $\boldsymbol{\pi} = \{\cdots, \Pr(\mathbf{Q} = [i, j]), \cdots\}$, the stationary probability of the queue length of each subqueue at ST is calculated as

$$\pi_1^i = \Pr(Q_1 = i) = \sum_{j=0}^{\infty} \Pr(\mathbf{Q} = [i, j]),$$

$$\pi_2^j = \Pr(Q_2 = j) = \sum_{i=0}^{\infty} \Pr(\mathbf{Q} = [i, j]). \tag{30}$$

With the derived $\boldsymbol{\pi}_i = \{\pi_i^0, \cdots, \pi_i^j, \cdots\}$, $i = 1, 2$, the queue performance, such as the average queue length and the average delay, of $ST1$ and $ST2$ can be calculated.

• Based on the probability theory, the average queue length of $ST1$ and $ST2$ equal to

$$N_{ST1} = \sum_{i=0}^{\infty} i\pi_1^i \quad \text{and} \quad N_{ST2} = \sum_{j=0}^{\infty} j\pi_2^j. \tag{31}$$

• According to Little's theorem, the average delay of packets in $ST1$ and $ST2$ can be calculated as

$$T_{ST1} = \frac{E[Q_1]}{\lambda_p} + E[X_{ST1}] \quad \text{and} \quad T_{ST2} = \frac{E[Q_2]}{\lambda_s} + E[X_{ST2}], \tag{32}$$

where $E[X_{ST1}]$ and $E[X_{ST2}]$ are average packet service times of $ST1$ and $ST2$, respectively, which can be calculated as $E[X_{ST-N}]$ similarly.

From the above analysis, it can be found that the size of the transition matrix is infinite. That is, the Matrix Solution Method, such as Gaussian Elimination, cannot be used and the numerical solution of $\boldsymbol{\pi}$ cannot be obtained. Hence, we assume that buffers of both $ST1$ and $ST2$ are finite and sizes of two buffers are B_1 and B_2, respectively. Then, applying Direct method or some typical Iterative methods, such as Power method and Jacobi's method, we can get the numerical solution of $\boldsymbol{\pi}$.

As proved in [27], under a stable situation, the assumption of no packets are dropped due to buffer overflow is acceptable. Hence, the error caused by the assumption of finite buffer size can be ignored. Furthermore, the buffer of the sensor is finite in practice. During calculating, if B_1 and B_2 choose small values, the numerical result may not be accurate. Meanwhile, larger B_1 and B_2 result in higher computation complexity, which requires that the device has strong computing capability. Hence, B_1 and B_2 should make a tradeoff between accuracy and computation complexity.

Combining the analysis of PT queue and $ST1$, the delay performance of the primary user can be calculated as

$$T_{PT-C} = T_{PT-Cp} + T_{ST1}. \tag{33}$$

V. NUMERICAL RESULTS

In this section, we will verify the analysis and study the queue performance of the system through simulation. Through comparing the results under different parameter sets, we find the relation between the queue performance and system parameters and the situation in which the cooperation can achieve better performance than the non-cooperation. During simulations, the received thresholds of PR, ST, and SR are 10dB. In figures, "Cooperation" and "NonCooperation" represent the system employing the cooperation between the primary user and the sensor or not, respectively. First, we observe the queue performance of the primary user and the WSN when $p_e = 1$. This is a special case where the sensor always has enough energy, and the influence of the energy harvesting is not considered. The average queue length and average delay are presented in Figs. 6-7.

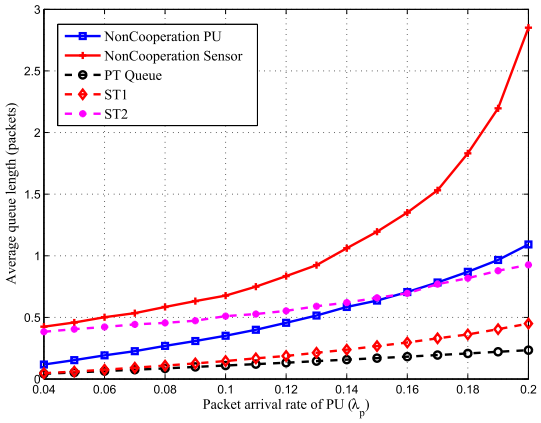

FIGURE 6. Average queue length varies with λ_p.

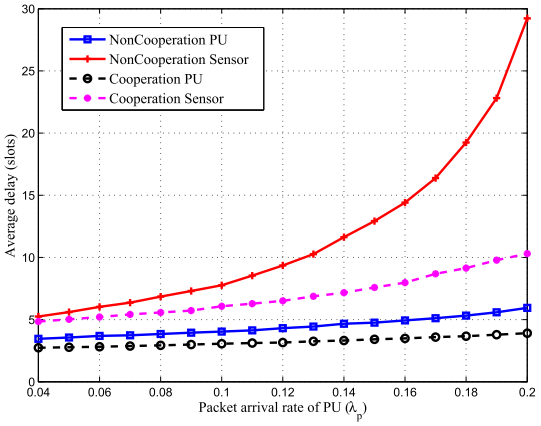

FIGURE 7. Average delay varies with λ_p.

In the simulation, the average SNR between PT and PR equals to the average SNR between ST and SR, which is 10dB, while $\bar{\gamma}_{sp} = \bar{\gamma}_{ps} = 25$dB. From Fig. 6, it can be found that the average queue length increases with increasing packet arrival rate of the primary user, especially the average queue length of the sensor in the system without cooperation. This result is consistent with the analysis in Sections III and IV. According to the above analysis, both N_{PT-N} in (3) and N_{ST-N} in (10) are proportional to λ_p. Furthermore, as the sensor works as a secondary user, from the point of view of the sensor, the traffic load increases faster than that of the primary user when the packet arrival rate of the primary user increases. Hence, the average queue length of the sensor increases significantly, especially when the cooperation is not adopted.

Fig. 7 illustrates the average packet delay of the sensor increases significantly while the increasing of the primary user's packet delay is not so apparent. As the same reason, the packet delay of the sensor in non-cooperation mode has the largest increasing rate. Moreover, the gap between the average delay in cooperation mode and non-cooperation is clearly expanding.

As shown in Figs. 6-7, in this situation, the performance of both the sensor and the primary user in cooperation mode is better than in non-cooperation mode. Hence, if the quality of the channel between the sensor and the primary user is better than the channel between the primary users, the cooperation should be adopted, especially when the packet arrival rate of the primary user is larger.

Then, we observe the influence of energy harvesting rate on the queue performance. The average queue length and the average packet delay are given in Figs. 8 and 9, respectively. The packet arrival rate of the primary user is 0.1 packets/slot while the energy harvesting parameter p_e changes from 0.1 to 0.5. With the increasing of p_e, the performance of the system is improved.

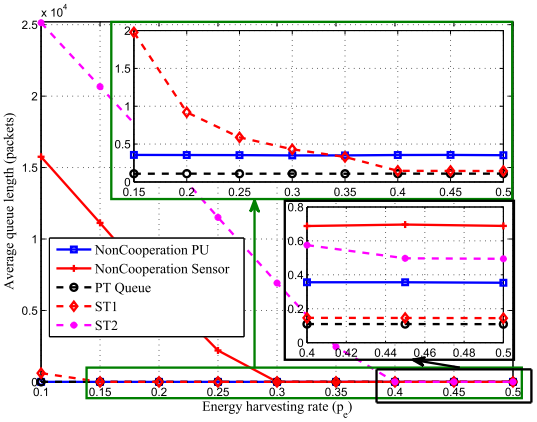

FIGURE 8. Average queue length varies with energy harvesting rate p_e.

From Fig. 8, it can be found that average queue lengths of three queues in the sensor decrease with the increasing p_e, especially the average queue length of the sensor in cooperation mode, which is denoted by ST2. Sub-figures in Fig. 8 show that $p_e = 0.4$ is a key value. When $p_e < 0.4$, the queue length of the sensor in non-cooperation mode is smaller than in cooperation mode. However, the result of $p_e \geq 0.4$ is just the opposite.

The result in 8 indicates that the delay performance of the system with the cooperation can be improved through increasing the energy harvesting rate. When $p_e \geq 4$, the delay performance of the primary user in cooperation mode is slightly less than in non-cooperation mode. Hence, through increasing energy harvesting rate (p_e), the delay performance of the primary user in cooperation mode can be improved, which may be even better than in non-cooperation mode. By integrating results in Figs. 8-9, we find that the queue performance of the system can be improved through increasing energy harvesting rate (p_e) when the energy harvesting rate is smaller than a certain value. If p_e reaches a certain value, the performance will be not influenced by p_e.

At last, we study the queue performance of system varies with the average SNR of channels between the sensor and the primary user under different p_e and $\gamma_p p$. During simulations, we set λ_p, λ_s, and $\bar{\gamma}_{ss}$ as 0.1, 0.2, and 15dB, respectively.

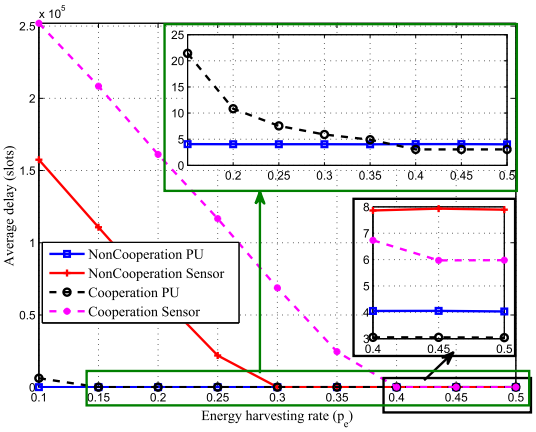

FIGURE 9. Average delay varies with energy harvesting rate p_e.

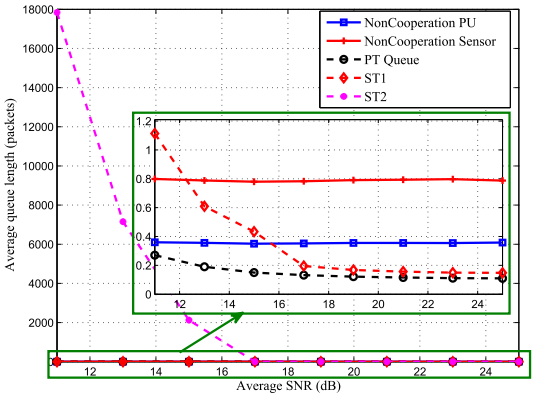

FIGURE 10. Average queue length varies with average SNR when $\bar{\gamma}_{pp} = 10$dB and $p_e = 0.4$.

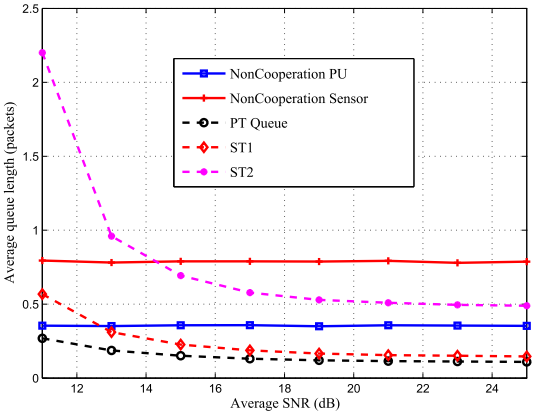

FIGURE 11. Average queue length varies with average SNR when $\bar{\gamma}_{pp} = 10$dB and $p_e = 0.6$.

The results are shown in Figs. 10-17. In Figs. 10-17, the x-axis is the average SNR between the sensor and the primary user. That is, $\bar{\gamma}_{sp}$ and $\bar{\gamma}_{ps}$.

When $\bar{\gamma}_{pp} = 10$dB, we first compare the average queue length of the system with $p_e = 0.4$ and $p_e = 0.6$, which are given in Figs. 10-11. As the result in Fig. 8, under the same channel quality, the energy harvesting energy can

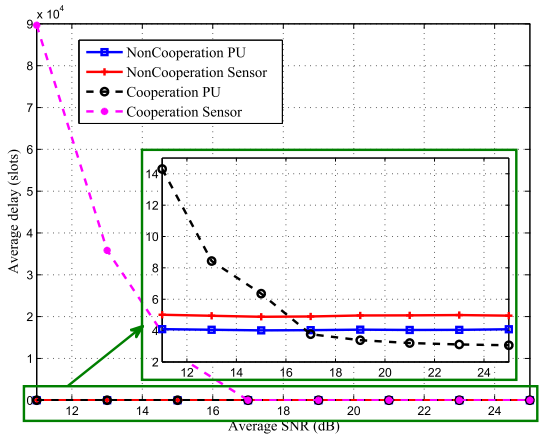

FIGURE 12. Average delay varies with average SNR when $\bar{\gamma}_{pp} = 10$dB and $p_e = 0.4$.

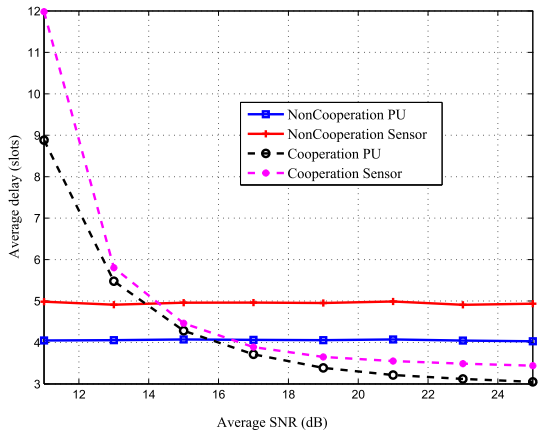

FIGURE 13. Average delay varies with average SNR when $\bar{\gamma}_{pp} = 10$dB and $p_e = 0.6$.

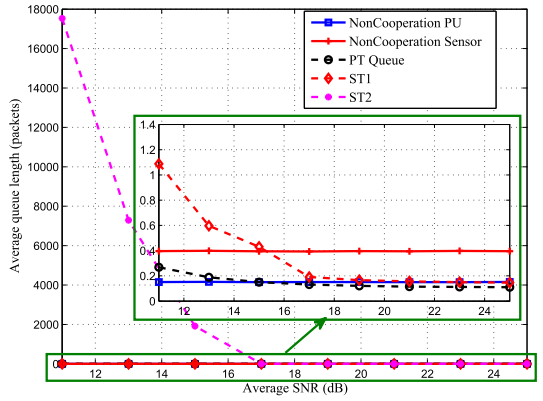

FIGURE 14. Average queue length varies with average SNR when $\bar{\gamma}_{pp} = 15$dB and $p_e = 0.4$.

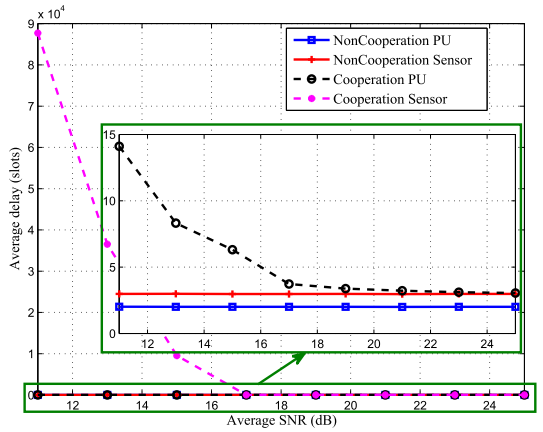

FIGURE 15. Average delay varies with average SNR when $\bar{\gamma}_{pp} = 15$dB and $p_e = 0.4$.

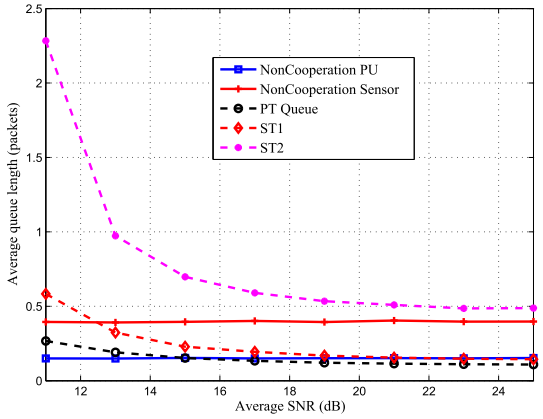

FIGURE 16. Average queue length varies with average SNR when $\bar{\gamma}_{pp} = 15$dB and $p_e = 0.6$.

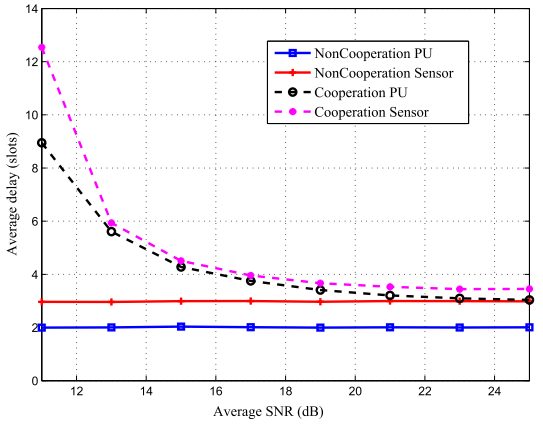

FIGURE 17. Average delay varies with average SNR when $\bar{\gamma}_{pp} = 15$dB and $p_e = 0.6$.

effectively improve the system performance, especially in cooperation mode. Beyond that, there is the same tendency of the average queue length with the increasing average SNR. As the primary user has higher priority, the average queue length of the queue in the primary user is little changed, which can be negligible. The average queue length of the queue in the sensor decreases with increasing average SNR, and the deceasing rate of ST2 is largest, when the average SNR is less than or equal to 15dB. If the average SNR is larger than 15dB, the performance is little changed and the sensor in cooperation mode achieves better queue performance.

The delay performance in Figs. 12 and 13 illustrates that the packet delay in cooperation mode decreases with increasing SNR while the packet delay in non-cooperation mode is constant. Under the condition $p_e = 0.4$, the delay of the primary user in cooperation mode is smaller than the delay in non-cooperation mode when the average SNR is larger than 17dB. The same phenomenon occurs in the situation with $p_e = 0.6$. Hence, the energy harvesting rate affects the absolute value of the packet delay while the average SNR influences the relative relation of the delay of the user working in different modes.

When the average SNR between PT and PR is 15dB, the queue performance of the system with different energy harvesting rates are given in Figs. 14-17. With the increasing of the average SNR between the sensor and the primary user, the queue performance is improved. However, neither of two users in cooperation mode can achieve the better performance than in non-cooperation mode. Furthermore, the sensor in cooperation mode has the worst performance, especially when the average SNR is smaller than 17dB. When $\bar{\gamma}_{ps}$ and $\bar{\gamma}_{sp}$ have smaller value, the packet transmission between the primary user and the sensor has lower successful probability, which results in less transmission chance of the sensor. Besides, the energy harvesting rate is small in this situation, thus the available energy of the sensor is limited. This limited energy and less transmission chance are used to relay packets of the primary user, thus packets of the sensor cannot be served timely. Comparing results in Figs. 10-15, there is an interesting phenomenon. No matter what the energy harvesting rate and the channel quality of the primary user, the queue performance of the system has little change after $\bar{\gamma}_{ps}$ and $\bar{\gamma}_{sp}$ are up to 17dB.

Comparing the result of the situation with $p_e = 0.4$, the performance of the system with cooperation is improved when the energy harvesting rate p_e is 0.6, and the tendency of the queue performance varying with the average SNR between the sensor and the primary user is similar. However, the queue performance of both the sensor and the primary user in cooperation mode is worse than in non-cooperation mode, even when the channel quality between the sensor and the primary user is better than the channel quality between PT and PR. In other words, the cooperation cannot improve the performance of the sensor in this situation. Hence, results in Figs. 14-17 indicate that the cooperation should not be adopted when the channel quality of primary user is not bad, such as the average received SNR is 15 dB, even if the energy is not a limitation.

VI. CONCLUSION

In this paper, we analyze the queue performance of the system consisting of an ENCRSN and primary users. The average queue length and average delay are derived. Through comparing the performance in cooperation mode and in noncooperation mode, we obtain the effect of system parameters on the queue performance and the condition under which the cooperation achieves better performance. Numerical results verify our analysis and indicate that energy harvesting rate and the channel condition between the sensor and primary user are two key influences. Furthermore, the influence of the primary user's packet arrival rate on the sensors is greater than on the primary user. These results are useful to design the quality of service of the EHCRSN.

REFERENCES

[1] Z. Su, Q. Xu, and Q. Qi, "Big data in mobile social networks: A QoE-oriented framework," *IEEE Netw.*, vol. 30, no. 1, pp. 52–57, Jan./Feb. 2016.

[2] R. Gunasagaran *et al.*, "Internet of Things: Sensor to sensor communication," in *Proc. IEEE SENSORS*, Nov. 2015, pp. 1–4.

[3] A. Sunny and J. Kuri, "A framework for designing multihop energy harvesting sensor networks," *IEEE J. Sel. Areas Commun.*, vol. 34, no. 5, pp. 1491–1501, May 2016.

[4] A. Ahmad, S. Ahmad, M. H. Rehmani, and N. Ul Hassan, "A survey on radio resource allocation in cognitive radio sensor networks," *IEEE Commun. Surveys Tuts.*, vol. 17, no. 2, pp. 888–917, 2nd Quart., 2015.

[5] J. Ren, Y. Zhang, R. Deng, N. Zhang, D. Zhang, and X. Shen, "Joint channel access and sampling rate control in energy harvesting cognitive radio sensor networks," *IEEE Trans. Emerg. Topics Comput.*, to be published.

[6] D. Zhang, Z. Chen, M. K. Awad, N. Zhang, H. Zhou, and X. S. Shen, "Utility-optimal resource management and allocation algorithm for energy harvesting cognitive radio sensor networks," *IEEE J. Sel. Areas Commun.*, vol. 34, no. 12, pp. 3552–3565, Dec. 2016.

[7] K. Zhang, Y. Mao, S. Leng, H. Bogucka, S. Gjessing, and Y. Zhang, "Cooperation for optimal demand response in cognitive radio enabled smart grid," in *Proc. IEEE Int. Conf. Commun. (ICC)*, May 2016, pp. 1–6.

[8] E. Ibarra, A. Antonopoulos, E. Kartsakli, J. J. Rodrigues, and C. Verikoukis, "QoS-aware energy management in body sensor nodes powered by human energy harvesting," *IEEE Sensors J.*, vol. 16, no. 2, pp. 542–549, Feb. 2016.

[9] J. Ren, J. Hu, D. Zhang, H. Guo, Y. Zhang, and X. Shen, "RF energy harvesting and transfer in cognitive radio sensor networks: Opportunities and challenges," *IEEE Commun. Mag.*, vol. 56, no. 1, pp. 104–110, Jan. 2018.

[10] J. Zheng, Y. Cai, X. Shen, Z. Zheng, and W. Yang, "Green energy optimization in energy harvesting wireless sensor networks," *IEEE Commun. Mag.*, vol. 53, no. 11, pp. 150–157, Nov. 2015.

[11] N. Zhang, H. Liang, N. Cheng, Y. Tang, J. W. Mark, and X. Shen, "Dynamic spectrum access in multi-channel cognitive radio networks," *IEEE J. Sel. Areas Commun.*, vol. 32, no. 11, pp. 2053–2064, Nov. 2014.

[12] Z. Chen, L. Guo, D. Zhang, and X. Chen, "Energy and channel transmission management algorithm for resource harvesting body area networks," *Int. J. Distrib. Sensor Netw.*, vol. 14, no. 2, pp. 1–14, 2018.

[13] S. K. Nobar, K. A. Mehr, J. M. Niya, and B. M. Tazehkand, "Cognitive radio sensor network with green power beacon," *IEEE Sensors J.*, vol. 17, no. 5, pp. 1549–1561, Mar. 2017.

[14] C. Xu, M. Zheng, W. Liang, H. Yu, and Y.-C. Liang, "End-to-end throughput maximization for underlay multi-hop cognitive radio networks with RF energy harvesting," *IEEE Trans. Wireless Commun.*, vol. 16, no. 6, pp. 3561–3572, Jun. 2017.

[15] S. Park, J. Heo, B. Kim, W. Chung, H. Wang, and D. Hong, "Optimal mode selection for cognitive radio sensor networks with RF energy harvesting," in *Proc. IEEE 23rd Int. Symp. Pers., Indoor Mobile Radio Commun. (PIMRC)*, Sep. 2012, pp. 2155–2159.

[16] T.-D. Le and O.-S. Shin, "Optimal relaying scheme with energy harvesting in a cognitive wireless sensor network," in *Proc. Int. Conf. Inf. Commun. Technol. Converg. (ICTC)*, Oct. 2016, pp. 82–84.

[17] F. Zhang, T. Jing, Y. Huo, and K. Jiang, "Outage probability minimization for energy harvesting cognitive radio sensor networks," *Sensors*, vol. 17, no. 2, p. 224, 2017.

[18] M. Ashraf, A. Shahid, J. W. Jang, and K.-G. Lee, "Optimization of the overall success probability of the energy harvesting cognitive wireless sensor networks," *IEEE Access*, vol. 5, pp. 283–294, 2017.

[19] Y. Zou, J. Peng, K. Liu, F. Jiang, and H. Lu, "Energy-efficent cooperative spectrum sensing for cognitive sensor networks with energy harvesting," in *Proc. Chin. Control Decis. Conf. (CCDC)*, May 2016, pp. 2373–2378.

[20] D. Zhang *et al.*, "Energy-harvesting-aided spectrum sensing and data transmission in heterogeneous cognitive radio sensor network," *IEEE Trans. Veh. Technol.*, vol. 66, no. 1, pp. 831–843, Jan. 2017.

[21] N. Jain and V. A. Bohara, "Energy harvesting and spectrum sharing protocol for wireless sensor networks," *IEEE Wireless Commun. Lett.*, vol. 4, no. 6, pp. 697–700, Jun. 2015.
[22] B. Cao, Q. Zhang, J. W. Mark, L. X. Cai, and H. V. Poor, "Toward efficient radio spectrum utilization: User cooperation in cognitive radio networking," *IEEE Netw.*, vol. 26, no. 4, pp. 46–52, Jul. 2012.
[23] S. K. Sharma, T. E. Bogale, S. Chatzinotas, B. Ottersten, L. B. Le, and X. Wang, "Cognitive radio techniques under practical imperfections: A survey," *IEEE Commun. Surveys Tuts.*, vol. 17, no. 4, pp. 1858–1884, 4th Quart., 2015.
[24] D. P. Bertsekas and R. G. Gallager, *Data Networks*, 2nd ed. Upper Saddle River, NJ, USA: Prentice-Hall, 1992.
[25] M. Sheng, W. Jiao, X. Wang, and G. Liu, "Effect of power control on performance of users in an interference-limited network with unsaturated traffic," *IEEE Trans. Veh. Technol.*, vol. 66, no. 3, pp. 2740–2755, Mar. 2017.
[26] G. Bolch, S. Greiner, H. de Meer, and K. S. Trivedi, *Queueing Networks and Markov Chains*. Hoboken, NJ, USA: Wiley, 2006.
[27] W. Jiao, M. Sheng, K.-S. Lui, and Y. Shi, "End-to-end delay distribution analysis for stochastic admission control in multi-hop wireless networks," *IEEE Trans. Wireless Commun.*, vol. 13, no. 3, pp. 1308–1320, Mar. 2014.

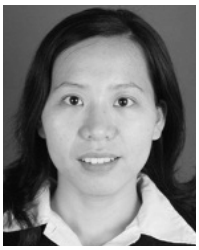

WANGUO JIAO received the B.S. degree in network engineering from Shijiazhuang Tiedao University, Shijiazhuang, China, in 2009, and the Ph.D. degree in telecommunication engineering from Xidian University, Xi'an, China, in 2015. Since 2015, she has been with the College of Information Science and Technology, Nanjing Forestry University, where she is currently an Assistant Professor. Her research interests include the performance analysis and protocol design of multi-hop wireless networks, cognitive radio networks, and wireless sensor networks with energy harvesting.

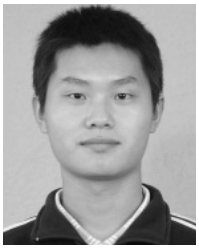

GUOQING LIU received the B.S. and Ph.D. degrees in telecommunication engineering from Xidian University, Xi'an, China, in 2005 and 2015, respectively. Since 2015, he has been with the Key Laboratory of IntelliSense Technology, China Electronics Technology Group Corporation, Nanjing Research Institute of Electronics Technology, where he is currently an Engineer. His research interests include wireless communication and radar.

HAIQING WU has been with the College of Information Science and Technology, Nanjing Forestry University, where she is currently an Associate Professor. Her research interests include the performance analysis and protocol design of wireless systems and sensor design for wireless sensor networks with energy harvesting.